Magnetic Orientation of Isotactic Polystyrene

Hidetoshi Ezure, Tsunehisa Kimura,* Shintaro Ogawa, and Eiko Ito

Department of Industrial Chemistry, Faculty of Engineering, Tokyo Metropolitan University, Minami-ohsawa, Hachioji, Tokyo 192-03, Japan

Received January 22, 1997; Revised Manuscript Received April 2, 1997[⊗]

ABSTRACT: Magnetic orientation of isotactic polystyrene during the isothermal crystallization at 210 °C in the magnetic field of 6 T is studied by using the magnetic birefringence, X-ray diffraction, and infrared measurements. The orientation starts in the vicinity of the end of the induction period, that is, before the crystal growth is observed by the wide angle X-ray diffraction This suggests that some anisotropic structures formed in the induction period are responsible for the magnetic orientation. Crystals formed are aligned with the *c*-axis, perpendicular to the magnetic field. Crystallization process is accelerted under the magnetic field.

Introduction

Polymeric materials can interact with a magnetic field through the diamagnetic anisotropy of constituent chemical units. The energy that the chemical unit gains through the interaction with an external magnetic field is dependent on the orientation of the unit relative to the magnetic field, and hence the unit tends to align to a certain direction in which the energy reduction is maximum. However, this tendency of the unit to align is suppressed by the thermal agitation, and the unit is unable to orient when the energy reduction is insufficient compared to the thermal energy. This is the case for nonliquid crystalline polymers in melts and solutions. Liquid crystalline polymers, on the other hand, form domains in which all the units are interrelated and responding to the magnetic field cooperatively. As a result, the reduction in the energy of the domain becomes large enough to overcome the thermal agitation. This is the explanation of the magnetic orientation of liquid crystalline polymers and low molecular weight liquid crystals,[1] as well as of crystals. There are a number of studies reporting the magnetic orientation of liquid crystalline polymers,[2−7] but few studies have been reported on the magnetic orientation of nonliquid crystalline polymers, except our previous work.[8]

The above picture suggests that a magnetic orientation does not occur in nonliquid crystalline polymers. However, we have found[8] that poly(ethylene-2,6-naphthalate), which is a semicrystalline polymer and is not regarded as a liquid crystalline polymer, undergoes a magnetic orientation during the heat treatment near the melting point. We believe that some ordered structures[9] are involved in this phenomenon. We assumed in the previous paper[8] that some ordered structures including a liquid-crystalline-like structure similar to that observed during the induction period of cold crystallization of poly(ethylene terephthalate)[10] and crystallites appearing during the crystallization process might be responsible for the magnetic orientation. On the basis of this assumption, it is expected that other crystalline polymers could also undergo a magnetic orientation. Actually, our preliminary study[11] demonstrated the magnetic orientation of isotactic polystyrene (*i*-PS). In this work, we report the magnetic orientation of *i*-PS during the isothermal melt crystallization studied by using the magnetic birefringence, X-ray diffraction, and infrared measurements.

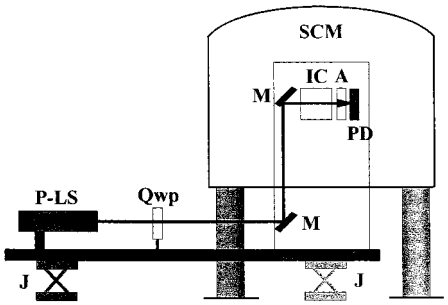

Figure 1. Block diagram of the optical apparatus for the magnetic birefringence measurements in a superconducting magnet: SCM, superconducting magnet; P-LS, polarized laser source; Q_{wp}, quarter wave plate; M, mirror; IC, insulating chamber; A, analyzer; PD, photo detector; J, jack.

Experimental Section

Material. Sample of *i*-PS purchased from Scientific Polymer Products, Inc., has nominal M_w of 400 000 and triad tacticity more than 90%. The melting point determined by differential scanning calorimetry (DSC) at the heating rate of 5 °C/min was 223 °C. Film samples were prepared by heat pressing the sample powder at 255 °C under 50 kg F/cm^2 for 2 min and quenched in the air. The thickness of the film was about 50 μm.

Apparatus for the Optical Measurement. The apparatus enables the measurement of the magnetic birefringence of polymer melts (up to 300 °C) in a superconducting magnet (89 mm in bore size and a vertical magnetic field of 6 T).[8,12] A block diagram of the apparatus is shown in Figure 1. By using two mirrors fixed inside an aluminum cylinder, a polarized He−Ne laser (632.8 nm, 1 mW, Meles Griot 05LHP111) beam is led to the top of the cylinder. The laser head is arranged such that the polarization plane at the top of the cylinder makes an angle of 45° to the magnetic field (crossed polars shown by (1) in Figure 2). Then the light goes into the analyzer, which makes an angle of 90° to the polarized light, and is finally detected by a photodetector. A quarter wave plate enables the rotation of the polarizing plane by 90° for a measurement under the parallel setting ((2) in Figure 2) is necessary. The laser head and the aluminum cylinder are fixed tightly on an aluminum frame, which is jacked up in order to insert the cylinder part into the bore of the superconducting magnet. A separable attachment is set on the top of the cylinder to provide a thermally insulated space (insulating chamber) in which a cylindrical sample heating cell is fixed in alignment with the laser beam. Figure 3 schematically shows the heating cell. A piece of sample film placed between

* To whom correspondence should be addressed.
[⊗] Abstract published in *Advance ACS Abstracts,* May 15, 1997.

S0024-9297(97)00077-6 CCC: $14.00

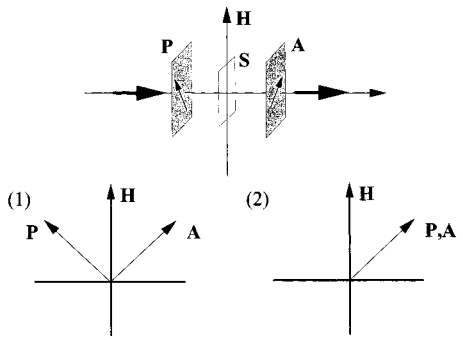

Figure 2. Optical geometry. The top shows the geometry of P, polarizing laser beam; A, analyzer; S, sample; and H, direction of the magnetic field, with the bottom displaying a setting of crossed polars (1) and a parallel setting (2).

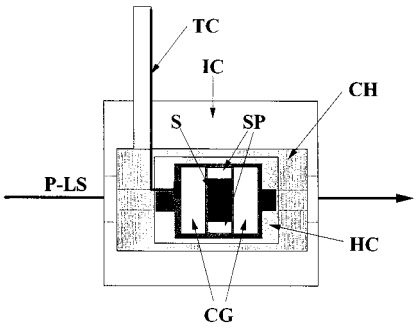

Figure 3. Schematic diagram of the heating cell: P-LS, polarized laser source; CG, cover glass; S, sample; SP, spacer; HC, heating cell; CH, coil heater; TC, thermocouple; IC, insulating chamber.

two round cover glasses (diameter of 10 mm) with a polyimide ring frame as a spacer is screwed into the cell. The plane of the cover glasses is parallel to the magnetic field and perpendicular to the laser beam. A chromelalumel thermocouple, calibrated for the measurement in the magnet, is set in touch with the one of the cover glasses. The calibration made based on the melting points of the lead and the tin indicates that the thermocouple in the magnet (6 T) shows a temperature about 3.8 °C higher than the actual temperature.

Optical Measurements and Sample Preparation. Measurements of the magnetic birefringence were carried out as follows: A heat-pressed film was set in the heating cell and heated at the heating rate of 5 °C/min from the room temperature to 255 °C, held at this temperature for 10 min to bring the sample to a melt, then cooled at the cooling rate of 5 °C/min down to a given temperature at which the sample undergoes the isothermal crystallization. The origin of the elapsed time of the isothermal crystallization was taken as the point where the sample temperature reaches the isothermal crystallization temperature. The above procedure was carried out all the way in the magnet. When it is necessary to obtain a sample for which the crystallization is truncated, the isothermal crystallization process was interrupted by rapidly cooling (ca. 100 °C/min) the heating cell with cold nitrogen gas. The film thus quenched was removed from the heating cell and peeled off from the round cover glasses to obtain a heat-treated specimen, which was subjected to the X-ray and infrared measurements. For comparison, exactly the same procedure was taken outside the magnet as well. The reproducibility of the measurement was about ±8 min with respect to the elapsed time of a peak position.

Optical Measurement with a Photomonitor. For the purpose of the temperature calibration of the optical apparatus, the change in the transmitting light intensity during the isothermal crystallization was recorded by using a photomonitor attached on an Olympus BH-2 microscope. The temperature was controlled by using a Mettler hot stage FP82HT system which was calibrated according to the instruction manual. A piece of a heat-pressed film sample was placed between two round cover glasses (the same condition as used in the optical apparatus) and was set on the hot stage. The thermal history given to the sample was the same as that given in the optical apparatus. The same microscope system was used for the measurement of the optical azimuthal scans of the quenched samples.

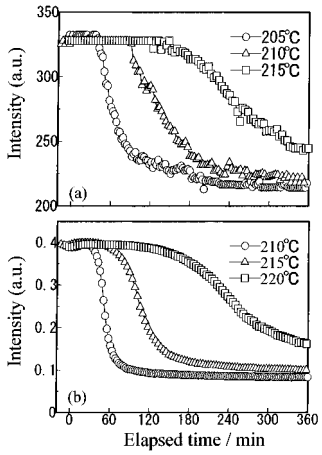

Figure 4. Comparison of the temporal change in transmitting light intensity under the parallel setting of the analyzer during the isothermal crystallization carried out with hot stage equipped with photomonitor (a) and with the optical apparatus (b) in order to calibrate the temperature of the optical apparatus. The temperatures indicate the crystallization temperatures: (a) the exact temperature and (b) temperatures indicated by the thermocouple in the heating cell (no correction). The figures indicate that the actual temperature of the sample in the optical apparatus is about 5 °C lower than the temperature indicated by the thermocouple in the heating cell.

Wide Angle X-ray Measurements. Wide angle X-ray diffraction (WAXD) measurements were carried out by using a MAC Science MXP system operating at 40 kV and 200 mA to generate a Ni-filtered Cu Kα X-ray beam. Azimuthal scans were carried out for the peak corresponding to (220) plane.[13,14]

Infrared Measurements. A Nicolet Magna750 was used for Fourier transform infrared (FT-IR) measurements with a resolution of 2 cm^{-1} and the number of scans being 100.

Temperature Calibration. Because of the limited space in the heating cell, the thermocouple cannot be inserted into the sample directly, but is set in touch with one of the round cover glasses as shown in Figure 3. This causes the deviation from the actual temperature of the sample. To estimate the difference, the temporal change in transmitting light intensity during the isothermal crystallization observed with the optical apparatus (outside the magnet) was compared with the light intensities obtained with the photomonitor. The parallel setting was used in both measurements, and hence the decrease in transmitting light intensity indicates the increase of the light scattered by some ordered structures. Figure 4 shows the temporal change in transmitting light intensity observed with the optical apparatus and the photomonitor. Comparing parts a and b, it is observed that the curves for the photomonitor obtained at 205, 210, and 215 °C are almost identical with the curves for the optical apparatus obtained at 210, 215, and 220 °C, respectively. Since the hot stage gives the exact temperature of the sample, the above observation indicates that the actual temperature of the sample is about 5 °C (more exactly 6 ± 1 °C) lower than the temperature indicated by the thermocouple in the heating cell. Therefore the following correction is made on the temperature values indicated by the thermocouple: correction by −5 °C for the measurement outside the magnet and by −8.8 °C for the measurement in the magnet. Hereafter the corrected temperature will be used whenever the measurements with the optical apparatus are concerned.

Results and Discussion

Optical and X-ray Measurements. Figure 5 displays the temporal change in the transmitting light

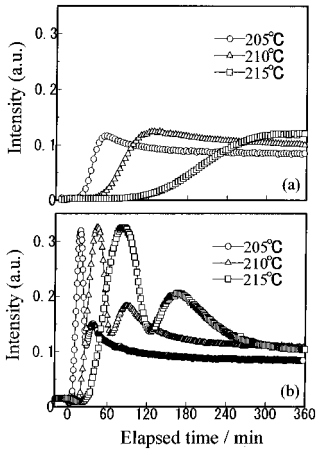

Figure 5. Temperature dependence of the temporal change in transmitting light intensity under crossed polars measured outside the magnet (a) and in the magnet (b). The temperatures indicate the isothermal crystallization temperatures.

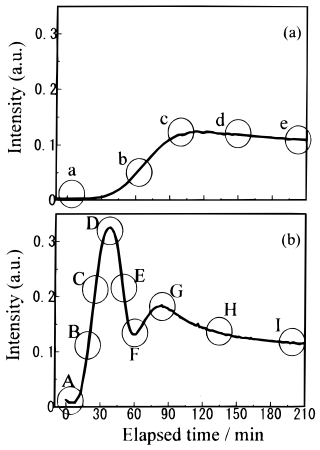

Figure 6. The points at which the isothermal crystallization at 210 °C is interrupted by a rapid cooling in order to obtain quenched samples in different stages of the orientation process: (a) outside the magnet and (b) in the magnet.

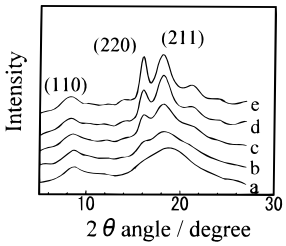

Figure 7. X-ray diffraction patterns of the samples quenched at different points of elapse time during the isothermal crystallization at 210 °C carried out outside the magnet. The alphabets attached correspond to those in Figure 6a. The intensity is reduced by sample thickness.

intensity measured under crossed polars during the isothermal crystallization at 205, 210, and 215 °C carried out in the magnet as well as outside the magnet. The increase in the intensity is attributed to the formation of anisotropic structures, such as crystallites, whether they are randomly oriented or aligned to the magnetic field. In the experiment with the magnetic field, the increase observed in the initial stage is due to the orientation of the anisotropic structure, as will be demonstrated later, while it is due to the random orientation of the anisotropic structure in the case of the measurement without the magnetic field. In the measurement with the magnetic field, the increase in the intensity starts at a shorter elapsed time at which no change is observed in the measurement without the magnetic field. Similar tendency is observed for all three temperatures studied here. The decrease in the intensity is attributed to the increase in the scattered light caused by the development of crystals. The reason for the appearance of the second maximum observed in the measurement with the magnetic field is not clear at present. However, a possible explanation is that the two maxima are attributed to the sinusoidal dependence of the intensity of the transmitting light I^2 on the change in the birefringence Δn, that is, $I^2 \sim \sin^2(\pi d \Delta n/\lambda)$, where d and λ are the sample thickness and the wave length of the light, respectively. The increase in the birefringence with the elapsed time results in the sinusoidal behavior of the intensity of the transmitting light.

In order to investigate the structure change during the crystallization process, the optical measurements at 210 °C were interrupted at different points of the elapsed time, and the specimen in the heating cell was quenched. The interruption points are indicated in Figure 6.

First, we present the X-ray results obtained for the experiments carried out outside the magnet. Figure 7 shows the X-ray diffraction patterns obtained for the samples quenched from the points a to e. At point a, zero elapsed time, no crystallites are observed. At the point b, a trace of crystalline structure seems to exist judging from small shoulders corresponding to the (220) and (211) planes.[13,14] With an increase in elapsed time, the crystallization proceeds and reaches the highest crystallinity at the point e. The differential scanning calorimetry measurement of the isothermal crystallization carried out with the same thermal history implies that the point b corresponds to the point slightly after the onset of the exothermic peak. We cannot locate the point b exactly on the corresponding point in the DSC thermogram because the simultaneous measurement is not available, but it could be said that the point b is located in the proximity of the onset of the exothermic peak. Combining the DSC and X-ray results, we could say that the point b is located between the end of the induction period and the start of crystallization. The sample b looks almost transparent with slight white haze on observation by eyes.

Next, we show the results of the measurement carried out in the magnet. The equatorial scans of the samples quenched at different points marked in Figure 6 by A through I are shown in Figure 8. Here, the equatorial direction is taken to the direction of the magnetic field. At the point A, zero elapsed time, no crystalline peak is observed. With increasing the elapsed time, crystallization proceeds. At the later stage of crystallization, the (211) peak is significantly small compared to the case without magnetic field. This suggests that the orientation of the *c*-axis is in the meridional direction (perpendicular to the magnetic field). The comparison of the diffraction patterns of the samples F and b, for example, which are both quenched at the elapsed time of about 60 min, clearly demonstrates that the crystallization is accelerated by the magnetic field. A similar conclusion will be drawn later on the basis of the infrared measurement. The growth rate and the morphology of crystals have been studied[15−17] for the *i*-PS crystallization from a melt in the case without magnetic fields, but little is known about the effect of the magnetic field. The similarity of the diffraction patterns for B and b indicates that the point B is located between the end of the induction period and the start of crystal-

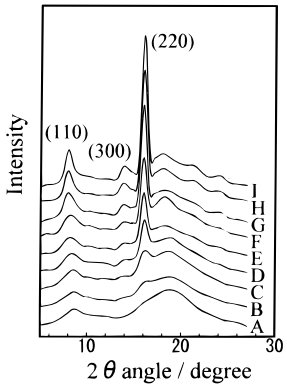

Figure 8. X-ray diffraction patterns of the samples quenched at different points of elapse time during the isothermal crystallization at 210 °C carried out in the magnet. The alphabets attached correspond to those in Figure 6b. The intensity is reduced by sample thickness. The equatorial direction is parallel to the magnetic field.

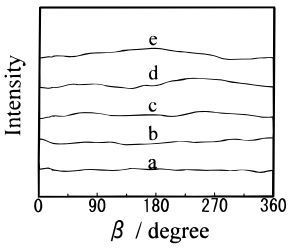

Figure 9. X-ray azimuthal scan along the (220) plane of the samples quenched at different points designated in Figure 6a (outside the magnet). The intensity is reduced by sample thickness.

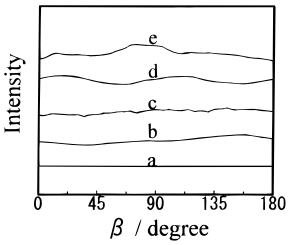

Figure 10. Optical azimuthal scan under corssed polars of the samples quenched at different points designated in Figure 6a (outside the magnet).

lization. This means that the induction period is reduced under the influence of the magnetic field since the elapsed time of the point B is far shorter than that of the point b. The sample B is almost transparent, with white haze less than that observed in sample b.

We now discuss about the orientation. Figure 9 displays the azimuthal scans carried out along the $2\theta = 16°$, corresponding to the (220) plane, for the samples quenched at the points a to e. Evidently, no orientation of crystallites is observed. The optical azimuthal scans measured with the photomonitor under crossed polars do not show the orientation either, as shown in Figure 10.

On the other hand, the magnetic orientation of the crystallites is clearly observed by means of the azimuthal scans along the (220) plane (Figure 11). The peaks around 90° and 270° are due to the crystallites aligned with the *c*-axis being perpendicular to the magnetic field. This direction of the orientation seems reasonable, considering relative directions of the phenyl rings of *i*-PS in 3_1 helical structure:[18,19] the planes of the phenyl rings pending from the helix are almost parallel to the direction of the magnetic field when the

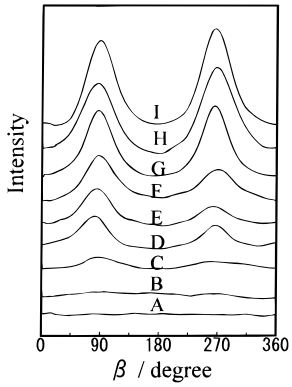

Figure 11. X-ray azimuthal scan along the (220) plane of the samples quenched at different points designated in Figure 6b (in the magnet). The intensity is reduced by sample thickness. The direction of the magnetic field is at $\beta = 0$ and 180°.

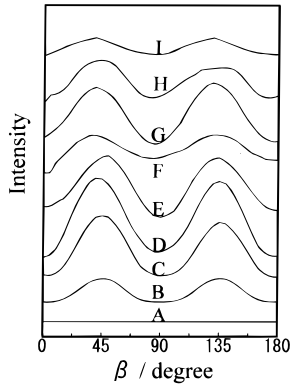

Figure 12. Optical azimuthal scan under crossed polars of the samples quenched at different points designated in Figure 6b (in the magnet). At $\beta = 0$ and 180°, the direction of the magnetic field is parallel to the analyzer.

helical axis lies perpendicular to the magnetic field. The peak height increases with the elapsed time, but the half width of the peak seems to remain unchanged. This suggests that the orientation is attained at the early stage of the orientation, followed by a subsequent crytal growth along the initial orientation. Though the diffraction of the sample B exhibits a shoulder at the position corresponding to (220) plane, as was mentioned previously, little sign is observed of the orientation of this plane. On the other hand, the optical measurement on the sample B with the photomonitor clearly exhibits the orientation as is shown in Figure 12. Therefore, the optical anisotropy observed at the point B is mainly attributed to the noncrystalline structure possibly including the liquid-crystal-like structure assumed in the induction period. As a matter of fact, the microscope observation of the sample B under crossed polars demonstrates that the transparent part exhibits the optical anisotropy.

Infrared Measurements. Figure 13 shows the infrared spectra of the samples for the points a to e. The assignments given in the literature[20−24] are used for the structure analyses. Bands at 899, 923, 1052, and 1083 cm^{-1} represent a regular 3_1 helix structure. The intensities of these bands depend on the sequence length of a regular helix structure. The separation of the 1052 and 1083 cm^{-1} bands is associated with the distortion of the regular helix structure: it is the largest in spectra of high crystalline samples and merges to a single peak at 1069 cm^{-1} in atactic polystyrene. In solution and amorphous bulk, the separation is intermediate. The band at 983 cm^{-1} reflects the intermolecular packing

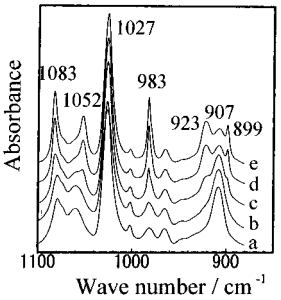

Figure 13. Infrared spectra of the samples quenched at different points designated in Figure 6a (outside the magnet).

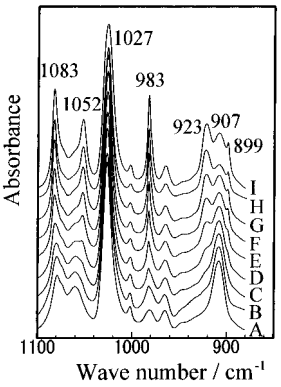

Figure 14. Infrared spectra of the samples quenched at different points designated in Figure 6b (in the magnet).

of the regular helix structure and is assigned to a crystal band.

Sample a does not show the crystal band at 983 cm^{-1}. A broad band at 981 cm^{-1} is common to all spectra and should be distinguished from the 983 cm^{-1} crystal band. Regular helix bands at 899, 923, 1052, and 1083 cm^{-1} are not observed. Instead, the bands assigned to the distorted helix are seen at 1060 and 1080 cm^{-1}. Also is seen a strong band at 907 cm^{-1}, which could be assigned to an amorphous band because atactic polystyrene, shows a band at this wave number. The sample b exhibits a small crystal band at 983 cm^{-1}. This coincides with the X-ray observation. In the figure, the regular helix bands are obscured by the distorted helix bands or the amorphous band, but the subtraction of the spectrum of sample a from that of sample b exhibits that the regular helix bands exist in the sample b. With increasing elapsed time, the crystal band becomes apparent in association with the regular helix bands.

Figure 14 shows the spectra for the points A to I. The temporal change of the spectrum profile is similar to that observed in Figure 13. The profile of the spectra B is very similar to that of the spectra b, which is in good agreement with the X-ray observation.

By using the 1027 cm^{-1} band intensity (I_{1027}) as the internal standard,[21] and the 983 cm^{-1} band intensity (I_{983}) as the measure of crystal, the crystal growth is evaluated in terms of the ratio I_{983}/I_{1027} (Figure 15). The figure shows that the magnetic field reduces the induction period and also causes a rapid growth in the initial stage of crystallization. This is in contrast to the crystallization without the magnetic field. In addition, the crystallinity is higher in the case with the magnetic field within the elapsed time covered in the present study.

Finally, we show the polarized infrared spectrum measured on the magnetically oriented sample (the point I) to confirm the direction of the molecular

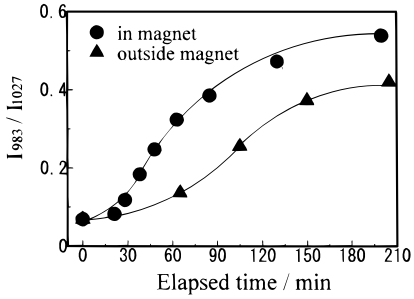

Figure 15. Crystal growth evaluated by the ratio of I_{983}/I_{1027}.

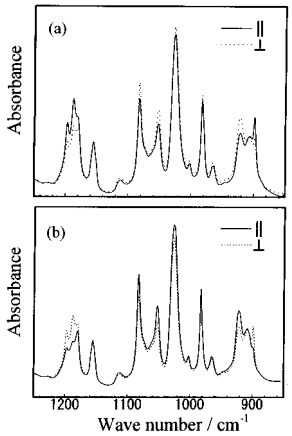

Figure 16. Polarized infrared spectra of (a) the sample uniaxially stretched and crystallized by annealing and (b) the magnetically oriented sample (the point (I)). Parllel symbols in (a) and (b) indicate that the polarization is parallel to the stretching direction and to the direction of the magnetic field, respectively.

orientation induced by the magnetic field. In Figure 16, the polarized infrared spectra for the sample I are shown along with those of an *i*-PS film uniaxially stretched and crystallized by annealing. Here, the parallel symbol indicates that the polarizing plane of the light is parallel to the direction of the magnetic field or to the stretching direction, while the perpendicular symbol indicates that the polarizing plane is perpendicular to the respective directions. Similarity of the stretched (∥, top) and magnetically aligned (⊥, bottom) spectra indicates that the direction perpendicular to the magnetic field corresponds to the stretching direction.

Conclusions

Magnetic orientation of *i*-PS is observed during the isothermal crystallization at 210 °C under the magnetic field of 6 T. The X-ray and infrared measurements for the samples quenched at various stages of the crystallization indicate that the orientation starts in the vicinity of the end of the induction period, that is, it starts before the peaks assignable to crystals in these measurements become significant. These observations lead to the conclusion that the liqiud-crystalline-like structure is most likely responsible for the magnetic orientation. However, this conclusion still needs to be tested on a larger number of systems: We do not rule out the possibility that crystallites in its very initial form are responsible for the orientation, and we do not know yet whether the liquid-crystalline-like structure persists after the induction period or it is just transient. On continuation of isothermal process, crystals grow and its *c*-axis lies perpendicular to the magnetic field. It is found that the induction period is reduced and the crystallization is accelerated under the magnetic field.

Acknowledgment. The authors express thanks to H. Sata for the calibration of the thermocouple in the magnet.

References and Notes

(1) de Gennes, P. G.; Prost, J. *The Physics of Liquid Crystals*, 2nd Ed.; Clarendon Press: Oxford, U.K., 1993.
(2) Krigbaum, W. R. *Polymer Liquid Crystals*; Academic Press: London, 1982; Chapter 10.
(3) Hardouin, F.; Achard, M. F.; Gasparoux, H.; Liebert, L.; Strzelecki, L. *J. Polym. Sci., Polym. Phys. Ed.* **1982**, *20*, 975.
(4) Anwer, A.; Windle, A. H. *Polymer* **1993**, *34*, 3347.
(5) Moore, J. S.; Stupp, S. I. *Macromolecules* **1987**, *20*, 282.
(6) Ito, E.; Sata, H.; Yamato, M. *Memoirs Fac. Technol., Tokyo Metrop. Univ.* **1993**, *43*, 4677.
(7) Kimura, T.; Maeda, T.; Sata, H.; Yamato, M.; Ito, E. *Polym. J.* **1995**, *27*, 247.
(8) Sata, H.; Kimura, T.; Ogawa, S.; Yamato, M.; Ito, E. *Polymer* **1996**, *37*, 1879.
(9) Brostow, W. *Physical Properties of Polymers Handbook*; Mark, J. E., Ed.; American Institute of Physics Press: New York, 1996; Chapter 33.
(10) Imai, M.; Kaji, K.; Kanaya, T.; Sakai, Y. *Phys. Rev. B.* **1995**, *52*, 12696.
(11) (a) Ezure, H.; Kimura, T.; Ogawa, S.; Ito, E. *Polym. Prep. Jpn.* **1996**, *45*, 841. (b) Ezure, H.; Kimura, T.; Ogawa, S.; Ito, E. *Polym. Prep. Jpn.* **1996**, *45*, 3081.
(12) Ogawa, S.; Kimura, T.; Sata, H.; Ezure, E.; Ito, E. *Rep. Progr. Polym. Phys. Jpn.* In press.
(13) Challa, G.; Hermans, P. H.; Weidinger, A. *Makromol. Chem.* **1962**, *56*, 169.
(14) Buchanan, D. R.; Miller, R. L. *J. Appl. Phys.* **1966**, *37*, 4003.
(15) Edwards, B. C.; Phillips, P. J. *Polymer* **1974**, *15*, 351.
(16) Suzuki, T.; Kovacs, A. *Polym. J.* **1970**, *1*, 82.
(17) Miyamoto, Y.; Tanzawa, Y.; Miyaji, H.; Kiho, H. *Polymer* **1992**, *33*, 2496.
(18) Bunn, C. W.; Howells, E. R. *J. Polym. Sci.* **1955**, *18*, 307.
(19) Natta, G.; Corradini, P.; Bassi, I. W. *Makromol. Chem.* **1958**, *28*, 166.
(20) Tadokoro, H.; Kitazawa, T.; Nozakura, S.; Murahashi, S. *Kobunshi Kagaku* **1960**, *17*, 231.
(21) Kobayashi, M.; Akita, K.; Tadokoro, H. *Makromol. Chem.* **1968**, *118*, 324.
(22) Kobayashi, M.; Tsumura, K.; Tadokoro, H. *J. Polym. Sci., Polym. Phys. Ed.* **1968**, *6*, 1493.
(23) Painter, P. C.; Koenig, J. L. *J. Polym. Sci., Polym. Phys. Ed.* **1977**, *15*, 1885.
(24) Kobayashi, M.; Nakaoki, T.; Ishihara, N. *Macromolecules* **1990**, *23*, 78.

MA970077G